Binding analysis of the Inositol-requiring enzyme 1 (IRE1) kinase domain

Antonio Carlesso[1], Chetan Chintha[2], Adrienne M. Gorman[2], Afshin Samali[2] and Leif A. Eriksson[1*]

[1]Department of Chemistry and Molecular Biology, University of Gothenburg, 405 30 Göteborg, Sweden

[2]Apoptosis Research Centre, National University of Ireland Galway, Galway, Ireland.

*Correspondence
Leif Eriksson, Department of Chemistry and Molecular Biology,
University of Gothenburg, 405 30 Göteborg, Sweden.
Email: leif.eriksson@chem.gu.se

SUPPLEMENTARY INFORMATION

Page

Table S1. Series of KIRA analogs (1−25)[1]. IRE1 kinase and RNase activity shown in half maximum inhibitory concentration (IC50) values (mean ± SEM, n = 3)[1].

Structure	BindingDB Ligand Name	Kinase IC50 (μm)	RNase IC50 (μm)	Reference
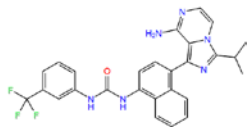	**Kira analogue 1**	**1.3 ± 0.1**	**1.8 ± 0.1**	[1]
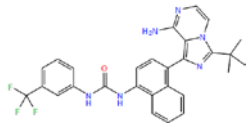	**Kira analogue 2**	**1.7 ± 0.02**	**0.12 ±0.01**	[1]
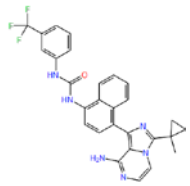	**Kira analogue 3**	**0.14 ± 0.01**	**0.090 ±0.01**	[1]
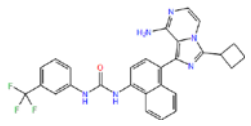	**Kira analogue 4**	**0.51 ± 0.04**	**0.18 ±0.04**	[1]
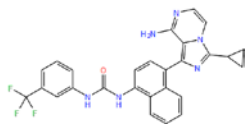	**Kira analogue 5**	**0.26 ± 0.01**	**0.48 ±0.02**	[1]

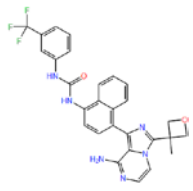	**Kira analogue 6**	**0.68 ± 0.06**	**0.33 ±0.01**	[1]
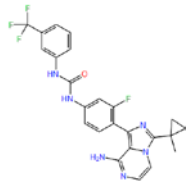	**Kira analogue 7**	**0.85 ± 0.05**	**0.39 ±0.01**	[1]
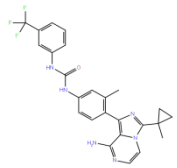	**Kira analogue 8**	**2.7 ± 0.5**	**1.5 ±0.1**	[1]
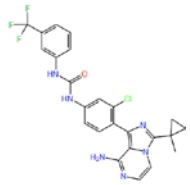	**Kira analogue 9**	**3.0 ± 0.2**	**2.4 ±0.1**	[1]
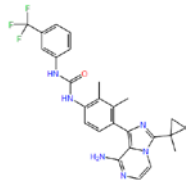	**Kira analogue 10**	**3.9 ± 0.2**	**1.2 ±0.1**	[1]

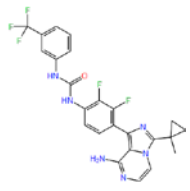	**Kira analogue 11**	**17 ± 1**	**20 ±5**	1
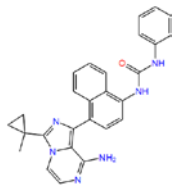	**Kira analogue 12**	**0.43 ± 0.07**	**0.19 ±0.01**	1
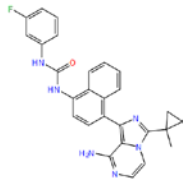	**Kira analogue 13**	**0.11 ± 0.01**	**0.22 ±0.01**	1
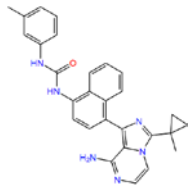	**Kira analogue 14**	**0.27 ± 0.03**	**0.26 ±0.01**	1
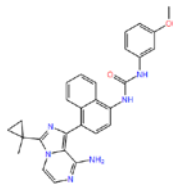	**Kira analogue 15**	**0.33 ± 0.08**	**0.31 ±0.01**	1

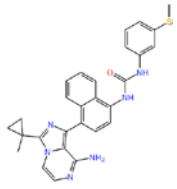	**Kira analogue 16**	**0.32 ±0.02**	**0.14 ±0.01**	[1]
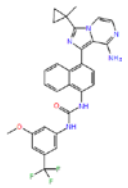	**Kira analogue 17**	**0.66 ±0.08**	**0.29 ±0.07**	[1]
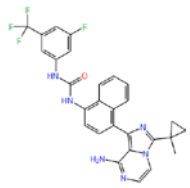	**Kira analogue 18**	**0.94 ± 0.06**	**0.61 ±0.07**	[1]
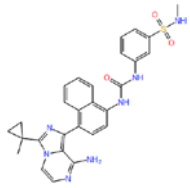	**Kira analogue 19**	**2.3 ± 0.7**	**1.6 ±0.1**	[1]
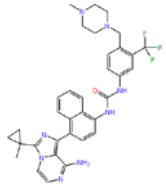	**Kira analogue 20**	**0.42 ± 0.14**	**0.19 ±0.05**	[1]

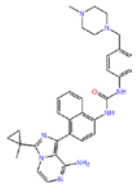	**Kira analogue 21**	**0.17 ± 0.07**	**0.34 ±0.02**	1
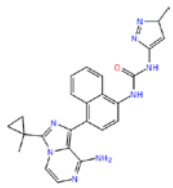	**Kira analogue 22**	**17 ± 5**	**7.1 ±3.0**	1
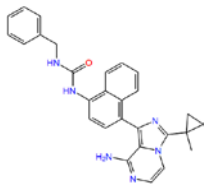	**Kira analogue 23**	**3.8 ± 0.8**	**3.8 ±0.8**	1
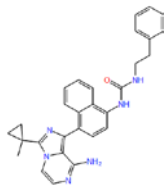	**Kira analogue 24**	**13 ± 1.7**	**13 ±1.7**	1
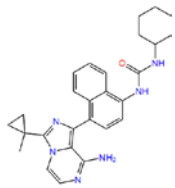	**Kira analogue 25**	**2.7 ± 0.4**	**2.7 ±0.4**	1
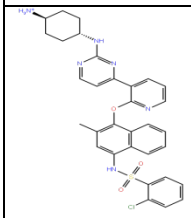	**KIRA analogue co-crystallized in 4U6R PDB structure**	**0.013**	**0.099**	5

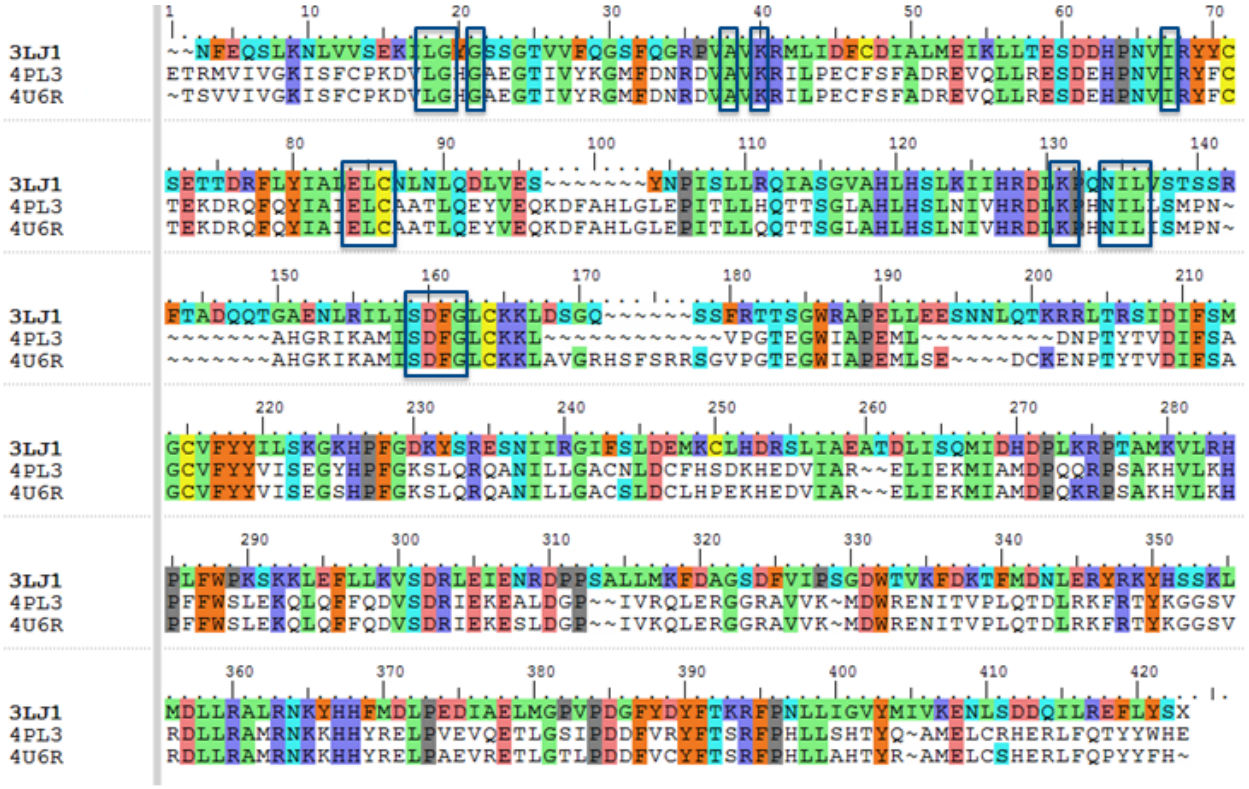

Figure S1. Sequence alignment of IRE1 cytosolic domain in different organism; yeast structure (PDB code: 3LJ1),murine (PDB code: 4PL3), and human (PDB code: 4U6R)using Bioluminate[2] in Schrödingher[3]. Identical residues are matched by same colour. Identical residues in the kinase active site, within a distance of 5.0 Å from the co-crystallized ligands, are highlighted using blue boxes.

```
CLUSTAL O(1.2.4) multiple sequence alignment


Aotus nancymaae     ------------------------GSSPTLEQDDGDEETSMVMVGKISFCPKDVLGHGAE      36
Pongo abelii        ------------------------GSSPSLEQDDGDEETSMVIVGKISFCPKDVLGHGAE      36
Homo sapiens        MGHNHRHKHHHHHHHHHENLYFQGPGSSPSLEQDDGDEETSVVIVGKISFCPKDVLGHGAE      60
Papio anubis        ------------------------GSSPSLEQDDGDEETSMVIVGKISFCPKDVLGHGAE      36
Piliocolobus t.     ------------------------GGSPSLEQDDGDEETSMVIVGKISFCPKDVLGHGAE      36
Ictidomys t.        -----------NHSLHSGSSVSKAGAGPFLEQDEEDEETSMVIVGKISFCPKDVLGHGAE      49
Felis catus         -----------NHSLHSSGSASRAGASPFLDQDDEDEETSMVIVGKISFCPKDVLGHGAE      49
Canis lupus f.      --------------------------PFLEQDDEDEETSMVIVGKISFCPKDVLGHGAE      33
                                             * *:**: *****:*:*****************


Aotus nancymaae     GTIVYRGMFDNRDVAVKRILPECFSFADREVQLLRESDEHPNVIRYFCTEKDRQFQYIAI      96
Pongo abelii        GTIVYRGMFDNRDVAVKRILPECFSFADREVQLLRESDEHPNVIRYFCTEKDRQFQYIAI      96
Homo sapiens        GTIVYRGMFDNRDVAVKRILPECFSFADREVQLLRESDEHPNVIRYFCTEKDRQFQYIAI     120
Papio anubis        GTIVYRGMFDNRDVAVKRILPECFSFADREVQLLRESDEHPNVIRYFCTEKDRQFQYIAI      96
Piliocolobus t.     GTIVYRGMFDNRDVAVKRILPECFSFADREVQLLRESDEHPNVIRYFCTEKDRQFQYIAI      96
Ictidomys t.        GTIVYRGMFDNRDVAVKRILPECFSFADREVQLLRESDEHPNVIRYFCTERDRQFQYIAI     109
Felis catus         GTIVYRGMFDNRDVAVKRILPECFSFADREVQLLRESDEHPNVIRYFCTERDRQFQYIAI     109
Canis lupus f.      GTIVYRGMFDNRDVAVKRILPECFSFADREVQLLRESDEHPNVIRYFCTERDRQFQYIAI      93
                    ************************************************:*********


Aotus nancymaae     ELCAATLQEYVEQKDFAHLGLEPITLLQQTTSGLAHLHSLNIVHRDLKPHNILISMPNAH     156
Pongo abelii        ELCAATLQEYVEQKDFAHLGLEPITLLQQTTSGLAHLHSLNIVHRDLKPHNILISMPNAH     156
Homo sapiens        ELCAATLQEYVEQKDFAHLGLEPITLLQQTTSGLAHLHSLNIVHRDLKPHNILISMPNAH     180
Papio anubis        ELCAATLQEYVEQKDFAHLGLEPITLLQQTTSGLAHLHSLNIVHRDLKPHNILISMPNAH     156
Piliocolobus t.     ELCAATLQEYVEQKDFAHLGLEPITLLQQTTSGLAHLHSLNIVHRDLKPHNILISMPNAH     156
Ictidomys t.        ELCAATLQEYVEQKDFAHLGLEPITLLQQTTSGLAHLHSLNIVHRDLKPHNILLSMPNAH     169
Felis catus         ELCAATLQEYVEQKDFAHLGLEPITLLQQTTSGLAHLHSLNIVHRDLKPHNILLSMPNAH     169
Canis lupus f.      ELCAATLQEYVEQKDFAHLGLEPITLLQQTTSGLAHLHSLNIVHRDLKPHNILLSMPNAH     153
                    ************************************************:******


Aotus nancymaae     GKIKAMISDFGLCKKLAVGRHSFSRRSGVPGTEGWIAPEMLSEDCKENPTYTVDIFSAGC     216
Pongo abelii        GKIKAMISDFGLCKKLAVGRHSFSRRSGVPGTEGWIAPEMLSEDCKENPTYTVDIFSAGC     216
Homo sapiens        GKIKAMISDFGLCKKLAVGRHSFSRRSGVPGTEGWIAPEMLSEDCKENPTYTVDIFSAGC     240
Papio anubis        GKIKAMISDFGLCKKLAAGRHSFSRRSGVPGTEGWIAPEMLSEDCKENPTYTVDIFSAGC     216
Piliocolobus t.     GKIKAMISDFGLCKKLAAGRHSFSRRSGVPGTEGWIAPEMLSEDCKENPTYTVDIFSAGC     216
Ictidomys t.        GRIKAMISDFGLCKKLAVGRHSFSRRSGVPGTEGWIAPEMLSEDCKENPTYTVDIFSAGC     229
Felis catus         GRIKAMISDFGLCKKLAVGRHSFSRRSGVPGTEGWIAPEMLSEDCKDNPTYTVDIFSAGC     229
Canis lupus f.      GRIKAMISDFGLCKKLAVGRHSFSRRSGVPGTEGWIAPEMLSEDCKDNPTYTVDIFSAGC     213
                    *:***************.****************************:**************


Aotus nancymaae     VFYYVISEGSHPFGKSLQRQANILLGACSLDSLHPEKHKDVIARELIEKMIAMDPQKRPS     276
Pongo abelii        VFYYVISEGSHPFGKSLQRQANILLGASSLDCLHPEKHEDVIARELIEKMIAMDPQKRPS     276
Homo sapiens        VFYYVISEGSHPFGKSLQRQANILLGACSLDCLHPEKHEDVIARELIEKMIAMDPQKRPS     300
Papio anubis        VFYYVISEGSHPFGKSLQRQANILLGACSLECLHPEKHEDVIARELIEKMIAMDPQKRPS     276
Piliocolobus t.     VFYYVISEGSHPFGKSLQRQANILLGACSLECLHPEKHEDVIARELIEKMIAMDPQKRPS     276
Ictidomys t.        VFYYVISEGSHPFGKSLQRQANILLGAYSLECFHPEKHEDVIARELIEKMIAMDPQQRPS     289
Felis catus         VFYYVISEGSHPFGKSLQRQANILLGAYSLDCLHPEKHEDVIARELIEKMIAMDPQKRPS     289
Canis lupus f.      VFYYVISEGSHPFGKSLQRQANILLGAYNLDCLHPEKHEDVIARELIEKMIAMDPQKRPS     273
                    *************************** .*:.:*****:*****************:***


Aotus nancymaae     AKHVLKHPFFWSLEKQLQFFQDVSDRIEKESLDGPIVKQLERGGRAVVKMDWRENITVPL     336
Pongo abelii        AKHVLKHPFFWSLEKQLQFFQDVSDRIEKESLDGLIVKQLERGGRAVVKMDWRENITVPL     336
Homo sapiens        AKHVLKHPFFWSLEKQLQFFQDVSDRIEKESLDGPIVKQLERGGRAVVKMDWRENITVPL     360
Papio anubis        AKHVLKHPFFWSLEKQLQFFQDVSDRIEKESLDGPIVKQLERGGRAVVKMDWRENITVPL     336
Piliocolobus t.     AKHVLKHPFFWSLEKQLQFFQDVSDRIEKESLDGPIVKQLERGGRAVVKMDWRENITVPL     336
Ictidomys t.        AKHVLKHPFFWSLEKQLQFFQDVSDRIEKESLDGPIVRQLERGGRAVVKMDWRENITVPL     349
Felis catus         AKHVLKHPFFWSLEKQLQFFQDVSDRIEKESLDGPIVKQLERGGRAVVKTDWRENITVPL     349
Canis lupus f.      AKHVLKHPFFWSLEKQLQFFQDVSDRIEKESLDGPIVKQLERGGRSVVKMDWRENITVPL     333
                    ********************************** **:********:*** **********


Aotus nancymaae     QTDLRKFRTYKGGSVRDLLRAMRNKKHHYRELPPEVRETLGSLPDDFVCYFTSRFPHLLA     396
Pongo abelii        QTDLRKFRTYKGGSVRDLLRAMRNKKHHYRELPAEVRETLGSLPDDFVCYFTSRFPHLLA     396
Homo sapiens        QTDLRKFRTYKGGSVRDLLRAMRNKKHHYRELPAEVRETLGTLPDDFVCYFTSRFPHLLA     420
Papio anubis        QTDLRKFRTYKGGSVRDLLRAMRNKKHHYRELPAEVRETLGSLPDDFVCYFTSRFPHLLA     396
Piliocolobus t.     QTDLRKFRTYKGGSVRDLLRAMRNKKHHYRELPAEVRETLGSLPDDFVCYFTSRFPHLLA     396
Ictidomys t.        QTDLRKFRTYKGGSVRDLLRAMRNKKHHYRELPVEVRETLGSLPDDFVRYFTSRFPHLLS     409
Felis catus         QTDLRKFRTYKGGSVRDLLRAMRNKKHHYRELPAEVRETLGSLPDDFVRYFTSRFPHLLP     409
Canis lupus f.      QTDLRKFRTYKGGSVRDLLRAMRNKKHHYRELPAEVRETLGSLPDDFVRYFTSRFPHLLS     393
```

```
                              ******************************** *******:****** **********

Aotus nancymaae      HTYRAMELCSHERLFQPYYFHEPLQPQPPVTPGAL  431
Pongo abelii         HTYQAMELCSHERLFQPYYFHEPPEPQPPVTPDAL  431
Homo sapiens         HTYRAMELCSHERLFQPYYFHEPPEPQPPVTPDAL  455
Papio anubis         HTYRAMELCSHERLFQPYYFHRPPEPQPPVTPDAL  431
Piliocolobus t.      HTYRAMELCSHERLFQPYYFHRPPEPQPPVTPDAL  431
Ictidomys t.         HTYRAMELCSHERLFQPYYFHEPLEPQPPVTPDAL  444
Felis catus          HTYRAMEPCSHERLFQPYYFHEPPELRPPVTPDAL  444
Canis lupus f.       HTYRAMEPCSHERLFQPYYFHEPPDTRPPVTPDTL  428
                     ***:*** *************.* : :*****.:*
```

Figure S2. A multiple sequence alignment of IRE1 cytosolic domain in 8 different organism using Clustal[4]. Residues are coloured as follow: AVFPMILW are shown in red, DE are blue, RHK are magenta, STYHCNGQ are green.

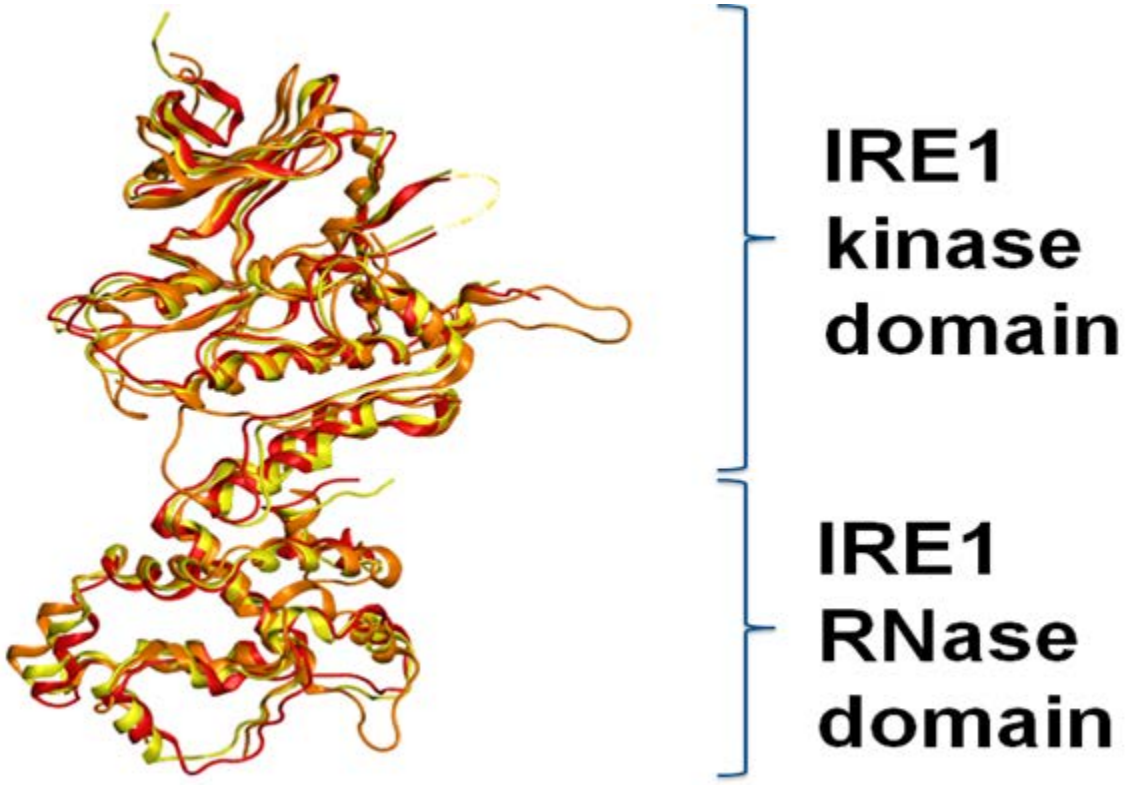

Figure S3. Superposition of the 3D structures of IRE1 in different organism; yeast structure in orange (PDB code: 2RIO), murine in yellow (PDB code: 4PL3), and human in red (PDB code: 5HGI).

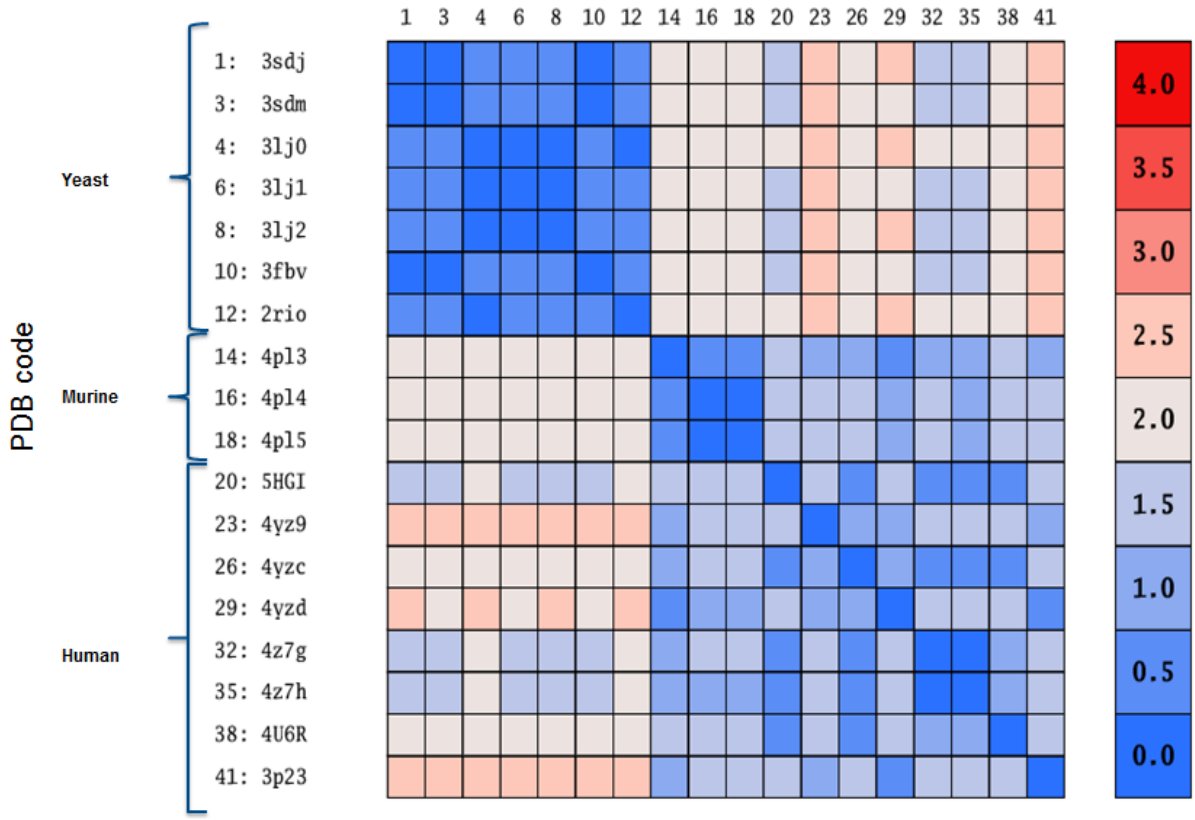

Figure S4. Root-mean-square deviation (RMSD) matrix values in Å of the positions of the Cα atoms for each pair of IRE1 cytosolic domain structures. The RMSD values are represented by a colorimetric scale, going from blue (0) to red (4.0).

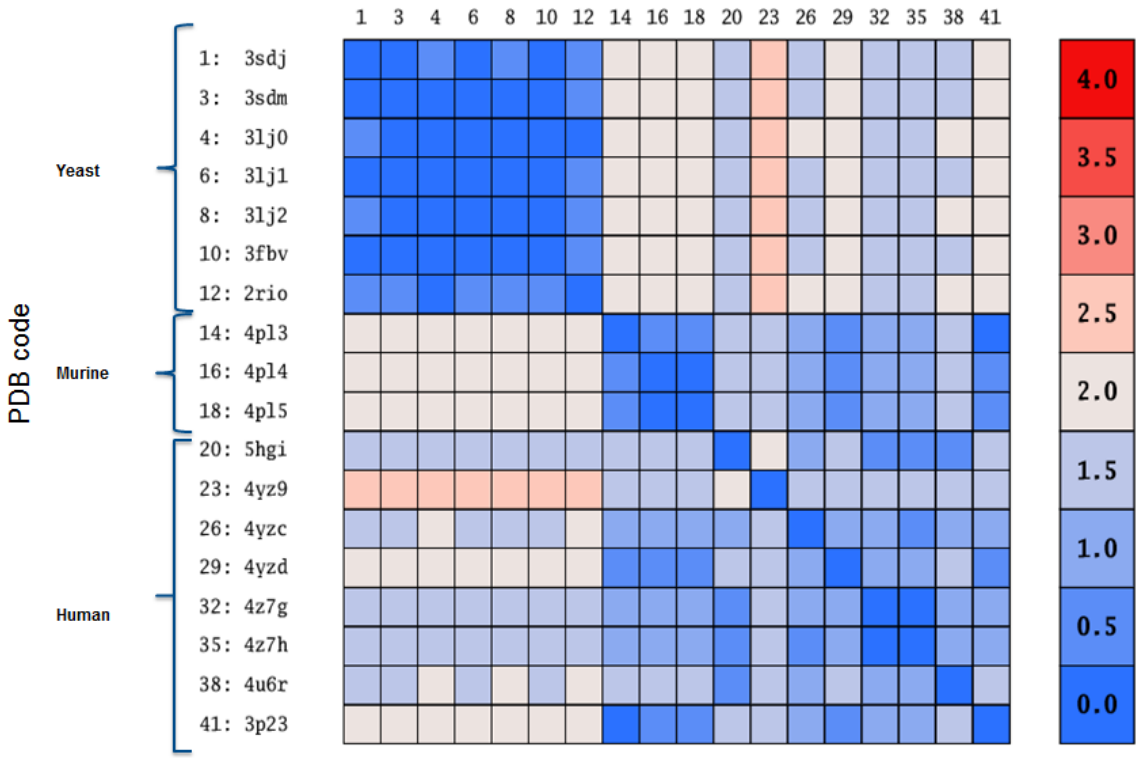

Figure S5. Root-mean-square deviation (RMSD) matrix values in Å of the positions of the Cα atoms for each pair of IRE1 kinase active site domain structures. The RMSD values are represented by a colorimetric scale, going from blue (0) to red (4.0).

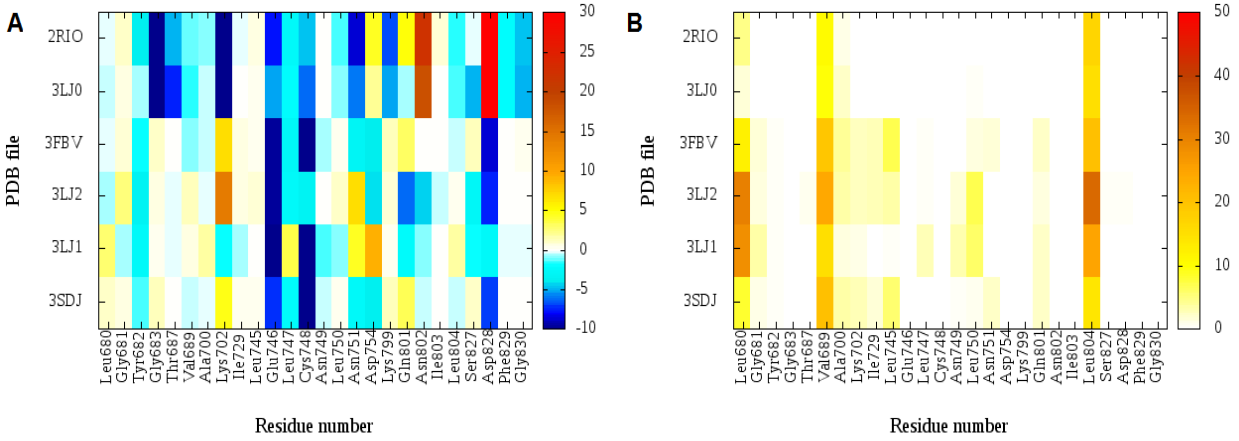

Figure S6. Per amino-acid interaction energy map for co-crystallized compounds inside the yeast IRE1 kinase binding site.

2RIO, 3LJ0: Endogenous ligands (ADP) co-crystallized on it;

3FBV, 3LJ2, 3LJ1 and 3SDJ: Exogenous ligands co-crystallized on it;

(A) Electrostatic energy values (kcal mol^{-1}). (B) Hydrophobic score (arbitrary units)

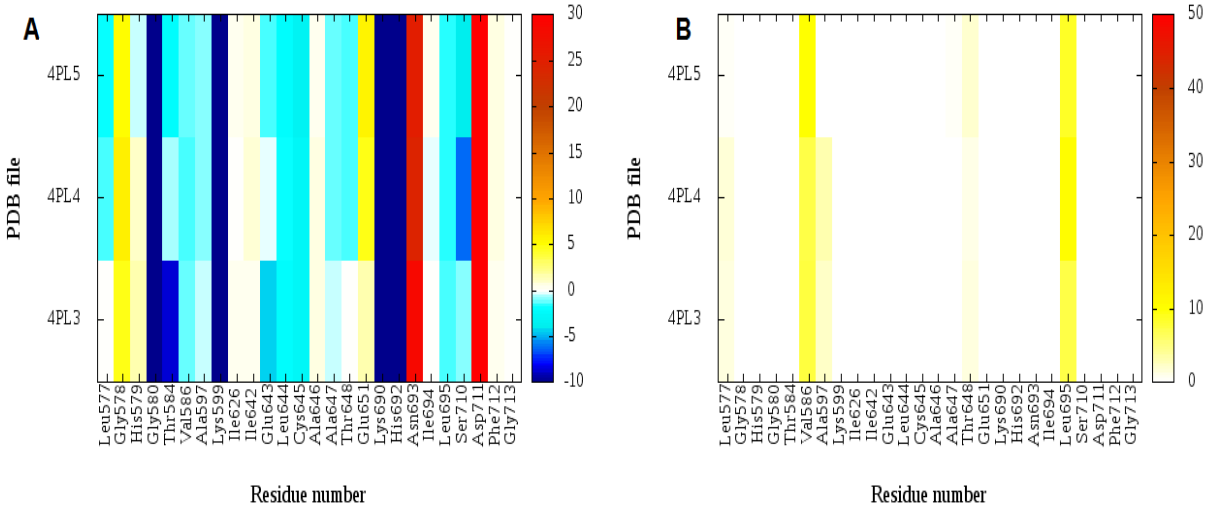

Figure S7. Per amino-acid interaction energy map for co-crystallized compounds inside the murine IRE1 kinase binding site.

A, B: Endogenous ligands (ADP)

(A) Electrostatic energy values (kcal mol^{-1}). (B) Hydrophobic score (arbitrary units)

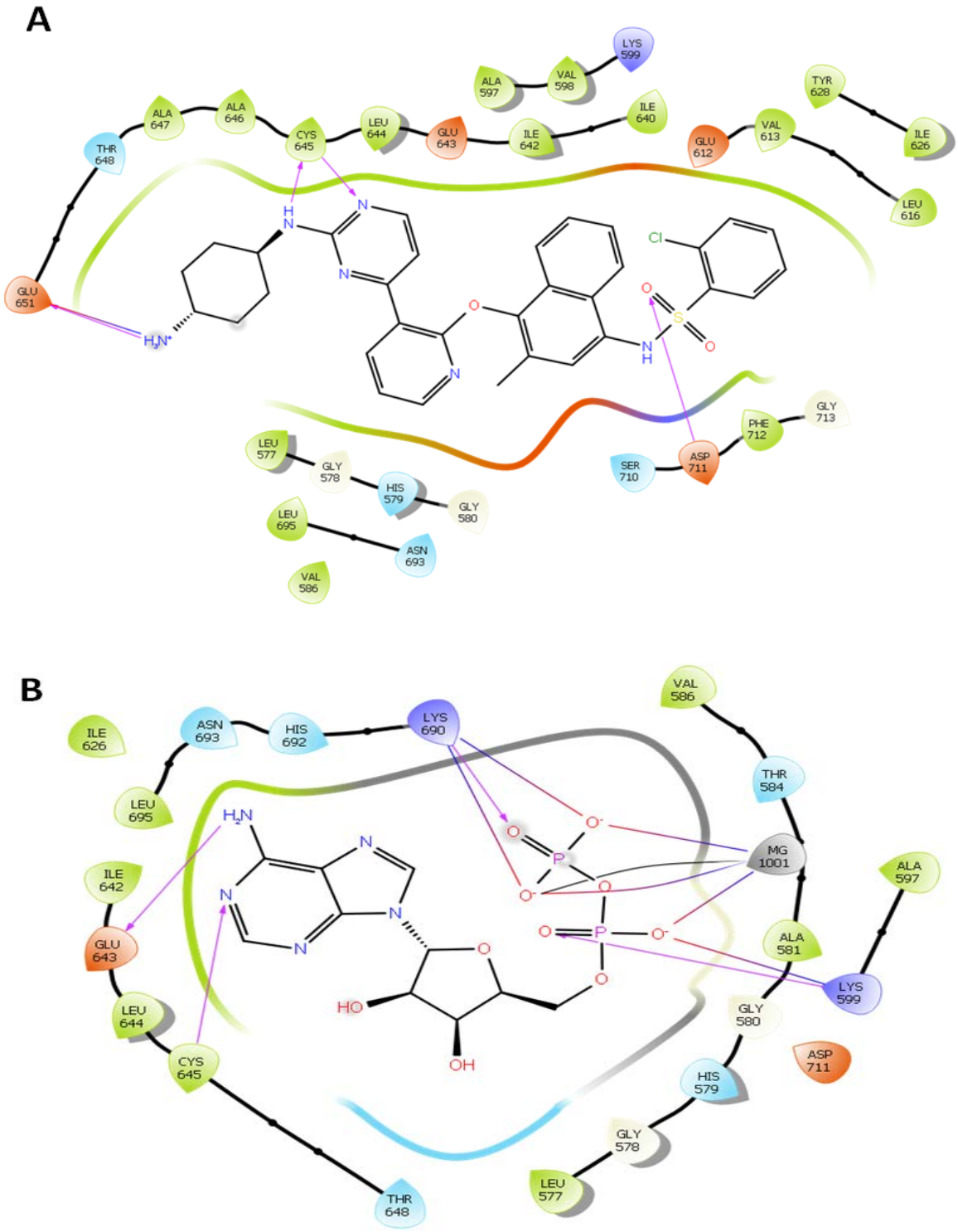

Figure S8. Schematic representation of the ligand interactions of (A) KIRA (PDB code: 4U6R) and (B) ADP (endogenous ligand) (PDB code: 3P23).

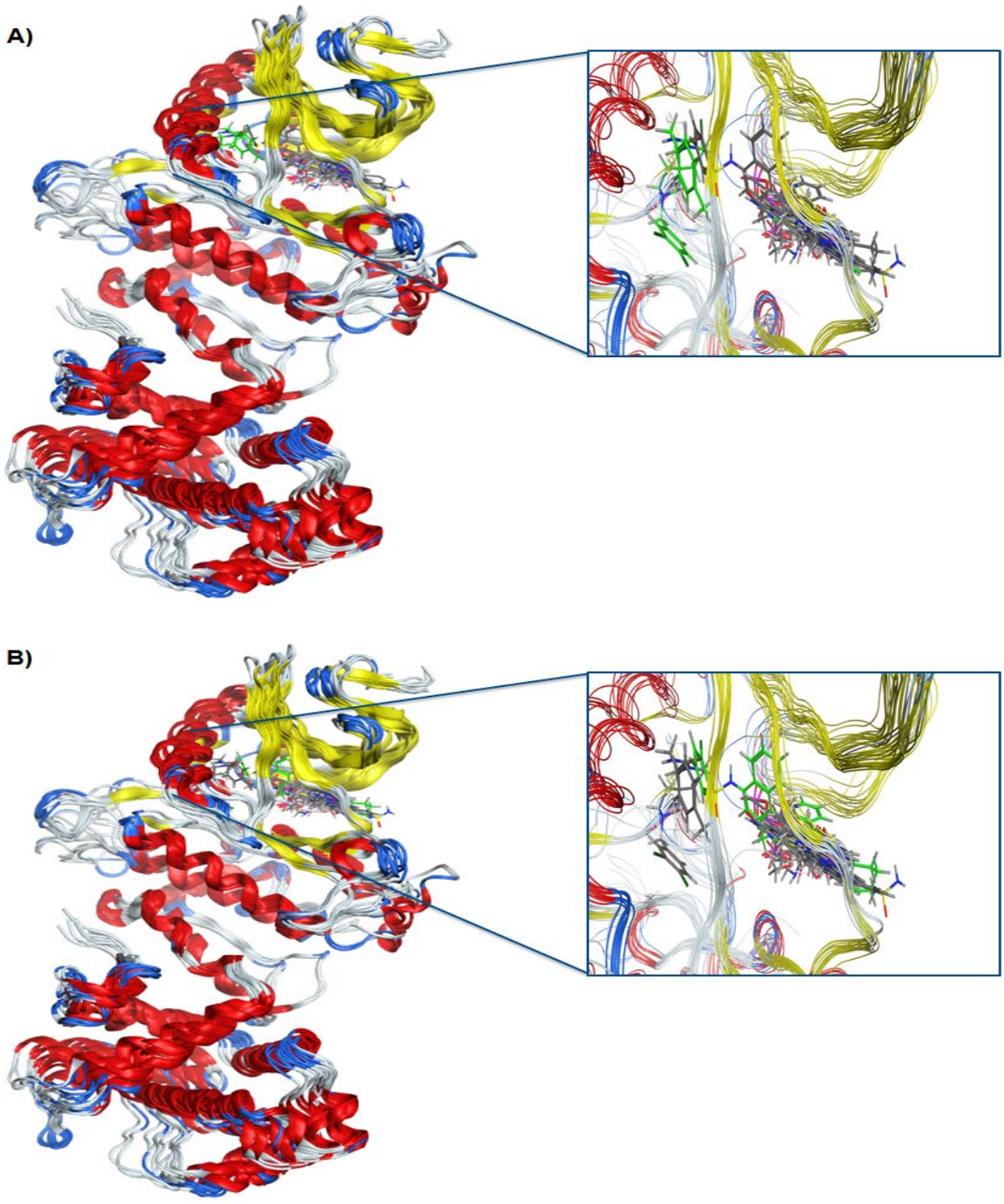

Figure S9. Superposition of all available 3D structures of IRE1 in different organism. Co-crystallized ligands are highlighted through stick representation: (A) Ligand co-crystallized in 4YZ9 PDB structure is coloured green, (B) Ligand co-crystallized in 4U6R PDB structure is coloured green.

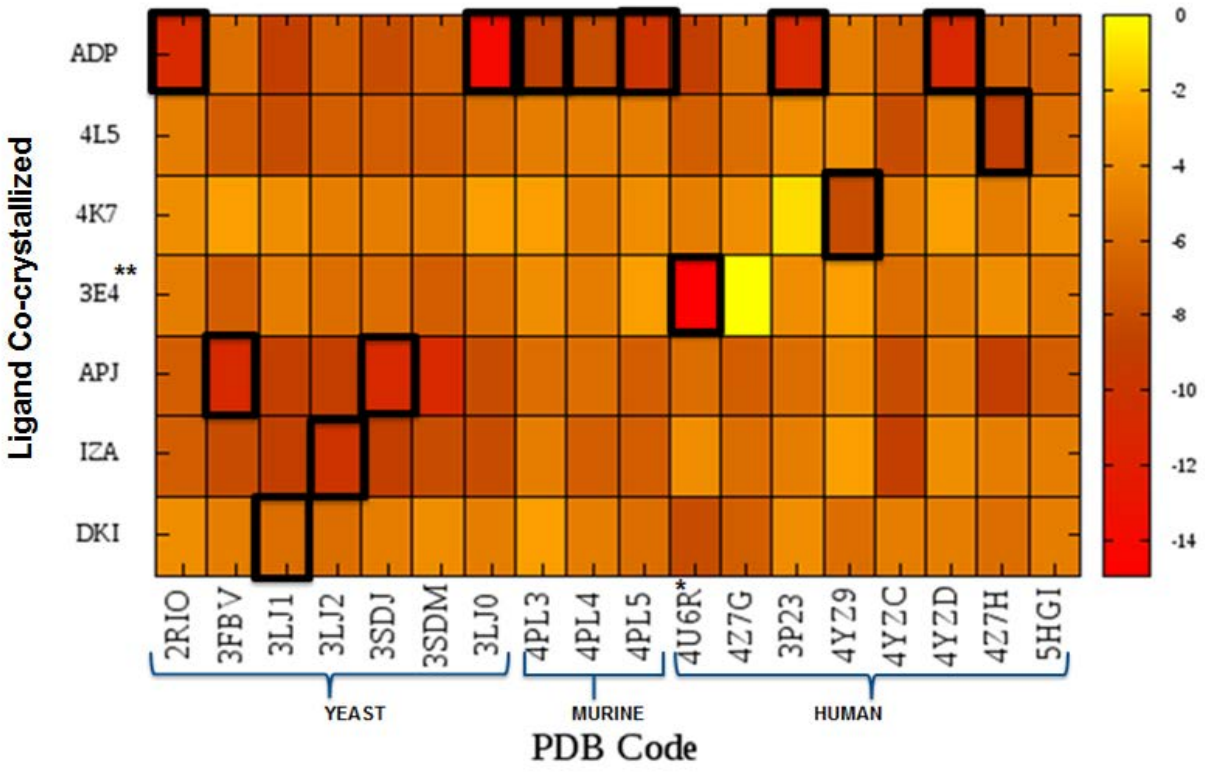

Figure S10. The Docking Score values returned by each co-crystallized ligand (y-values) for each IRE1 PDB structure (x-values) are represented by a colorimetric scale, going from red (-15) to yellow (0) indicative of Docking score value. Co-crystallized ligands highlighted with boxes for each IRE1 structure. *Dephosphorylated IRE1α co-crystallized with KIRA[1]. **KIRA co-crystallized in 4U6R PDB structure.

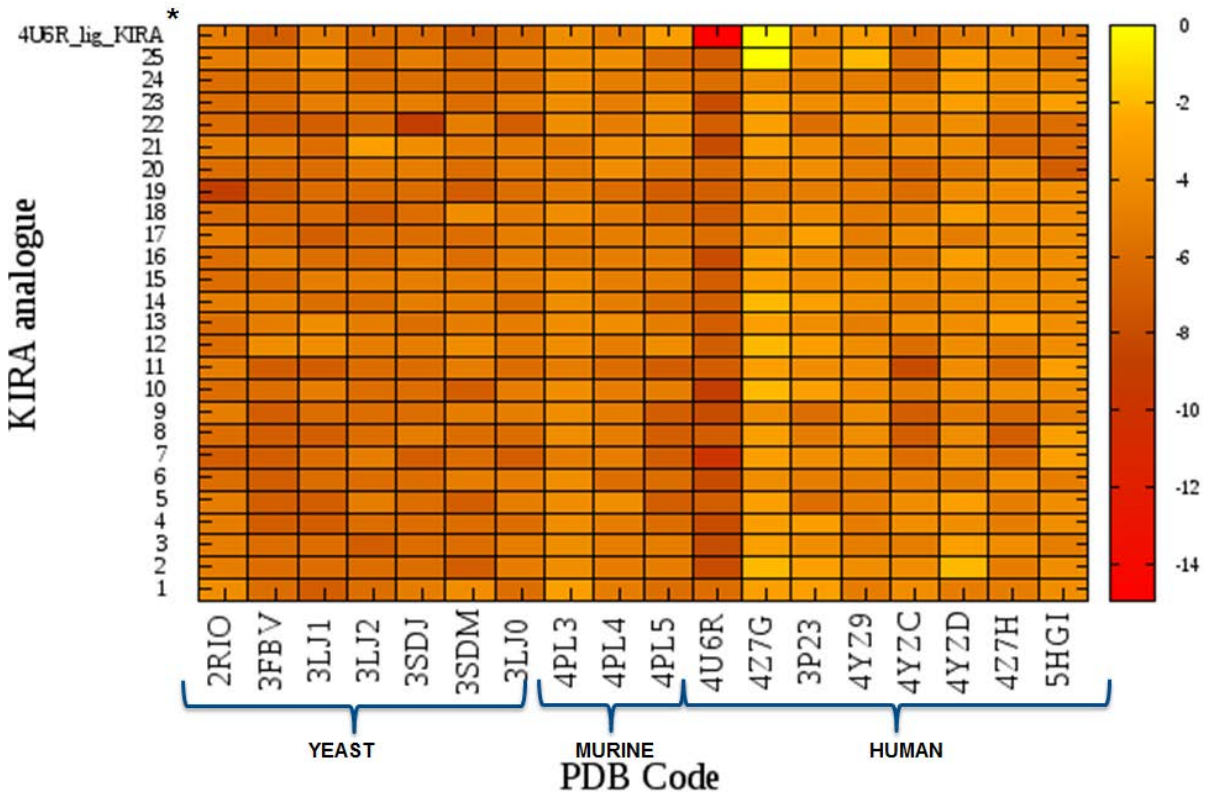

Figure S11. The Docking Score of each KIRA analogues (y-values1-25) for each IRE1 PDB structures (x-values) are represented by a colorimetric scale, going from red (-15) to yellow (0) indicative of Docking score value. *KIRA co-crystallized in 4U6R PDB structure.

Bibliography

(1) Feldman, H. C.; Tong, M.; Wang, L.; Meza-Acevedo, R.; Gobillot, T. A.; Lebedev, I.; Gliedt, M. J.; Hari, S. B.; Mitra, A. K.; Backes, B. J.; et al. Structural and Functional Analysis of the Allosteric Inhibition of IRE1α with ATP-Competitive Ligands. *ACS Chem. Biol.* **2016**, *11* (8), 2195–2205.

(2) Schrödinger Release 2015-4: BioLuminate, Schrödinger, LLC, New York, NY, 2015.

(3) Schrödinger Release 2015-4: Maestro, Schrödinger, LLC, New York, NY 2015.

(4) Chenna, R.; Sugawara, H.; Koike, T.; Lopez, R.; Gibson, T. J.; Higgins, D. G.; Thompson, J. D. Multiple Sequence Alignment with the Clustal Series of Programs. *Nucleic Acids Res.* **2003**, *31* (13), 3497–3500.

(5) Harrington, P. E.; Biswas, K.; Malwitz, D.; Tasker, A. S.; Mohr, C.; Andrews, K. L.; Dellamaggiore, K.; Kendall, R.; Beckmann, H.; Jaeckel, P.; et al. Unfolded Protein Response in Cancer: IRE1α Inhibition by Selective Kinase Ligands Does Not Impair Tumor Cell Viability. *ACS Med. Chem. Lett.* **2015**, *6* (1), 68–72.